ACS APPLIED MATERIALS & INTERFACES

Letter

www.acsami.org

Rapid Microwave Synthesis of Graphene Directly on *h*-BN with Excellent Heat Dissipation Performance

Tianquan Lin,[†] Zhanqiang Liu,[†] Mi Zhou,[†] Hui Bi,[†] Ketian Zhang,[‡] Fuqiang Huang,*[,†,‡] Dongyun Wan,[†] and Yajuan Zhong[†]

[†]CAS Key Laboratory of Materials for Energy Conversion, Shanghai Institute of Ceramics, Chinese Academy of Sciences, Shanghai 200050, China

[‡]State Key Laboratory of Rare Earth Materials Chemistry and Applications, College of Chemistry and Molecular Engineering, Peking University, Beijing 100871, China

Supporting Information

ABSTRACT: We report a new rapid household microwave method to successfully grow graphene on *h*-BN flakes without using any catalysts. We obtained a novel uniform multilevel matrix of vertical graphene sheets on *h*-BN flakes. The unique structure possessed outstanding electron conductivity and thermal properties (29.1 W m^{-1} K^{-1}).

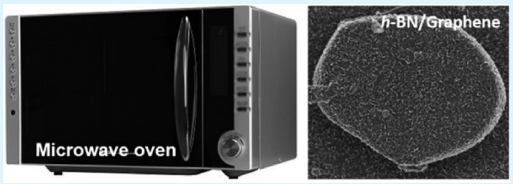

KEYWORDS: *graphene, h-BN, heat dissipation, microwave-assisted synthesis, rapid growth*

The heat dissipation problem in microelectronic circuits is becoming increasingly important as the demands in denser and faster circuits intensify. The high thermal conductivity can be achieved by the use of suitable electrically insulating fillers such as alumina, boron nitride, and alumina nitride or other ceramic powders.[1] Hexagonal boron nitride (*h*-BN) has high thermal conductivity and excellent high temperature resistance, together with lightweight and moderate cost, compared with other ceramic heat sinks.[2,3] However, because of the large thermal resistance between *h*-BN, the superior performance of individual *h*-BN crystal is not well represented, in terms of electrical conductivity and thermal conductivity. In addition, one of the most well-known characteristics of *h*-BN is the very bad wettability by metal melts (like Al, Mg, Zn, Pb, and Cu).[4]

Carbon allotropes and their derivatives occupy a unique place in terms of their ability to conduct heat.[5] The superb thermal conduction property of graphene (~5000 W m^{-1} K^{-1})[6] makes it an excellent material for thermal management and is beneficial for electronic applications.[7−9] The extremely high thermal conductivity can make graphene be used to improve the thermal properties of ceramics.[10] On the other hand, *h*-BN is an isoelectric analogue of graphite, which has been considered as one of the best substrates to maintain the excellent transport behaviors of graphene.[11,12] A hybrid consisting of *h*-BN and graphene is another interesting structure that would enable the tailoring of physical properties in graphene-based structures.[13,14] The wettability is excellent between graphene and metals due to strong interaction of the π orbitals of the graphene layer with the *d* orbitals of the metals.[15] Therefore, when combined with graphene, *h*-BN will acquire high interfacial thermal conductivity and good wettability with metals. This requires direct growth of graphene on *h*-BN to maintain the excellent interfacial thermal and electronic conductivities. The graphene layer has been directly grown by chemical vapor deposition (CVD) onto an *h*-BN (0001) monolayer substrate on Ru (0001) and Ni (111) surfaces.[14,16,17] These CVD graphene preparations need to be assisted by the transition metal catalysts, which are highly undesired. The direct growth of hybrid graphene on *h*-BN material remains to be highly challenging.

For the most part, conventional thermal techniques rely on conduction of blackbody radiation to drive there action. The reaction vessel acts as an intermediary for energy transfer from the heating mantle to the solvent and finally to the reactant molecules. This can cause sharp thermal gradient and inefficient, nonuniform reaction conditions.[4] Microwave synthesis is a very promising preparation method for many materials, such as semiconductors,[18] superconductors,[19] ceramics,[20] and carbon derivatives,[21] and for reduction of graphene oxide,[20,22−24] because it is fast, clean and energy efficient.[20] Microwave dielectric heating not only enhances the rate of formation, it also enhances the material quality and size distributions.[4]

In this research, we report a new method to grow graphene directly on *h*-BN crystals using a 700 W household microwave oven for only 5 min, as illustrated in Figure 1. In a typical synthesis, *h*-BN crystal flakes (0.1 g, whose typical size ranges in 20−50 μm as shown in Figure S1 in the Supporting Information) were dispersed in 5 mL of polymethylmethacrylate (PMMA, 4 wt % in anisole solution), and dried in a vacuum oven at 100 °C for 6 h to obtain the PMMA-coated *h*-

Received: December 10, 2013
Accepted: February 20, 2014
Published: February 20, 2014

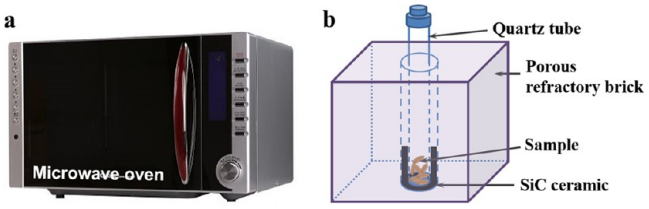

Figure 1. (a, b) Scheme of the microwave-assisted synthesis for graphene on *h*-BN using solid carbon source.

BN flakes. These PMMA-coated *h*-BN flakes were evacuated in quartz tubes (~500 Pa). The sealed quartz tubes were wrapped by microwave transparent porous refractory ceramics in order to reduce thermal radiation loss. The whole assembly was put into a household microwave oven (Galanz P70D20TLK-D4, Frequency 2.45 GHz) for graphene growth. Here, the SiC ceramic board was placed underneath the silica tube as a heat reservoir because of its high efficiency for microwave absorption and providing the thermal energy for graphene growth.

Few-layer graphene sheets directly grown on *h*-BN samples derived from 4 wt.% PMMA were first investigated by scanning electron microscope (SEM) as shown in Figure 2a–c. The first novelty of our study is that graphene has a continuous flower-like structure beyond the *h*-BN substrates rather than a conventional grown only along the *h*-BN plane. The morphology of graphene growth on *h*-BN was further observed by transmission electron microscope (TEM), as shown in Figure 2d. The graphene sheets are around the *h*-BN flakes. The graphene nanosheets grew along the *h*-BN plane and then extended out above or beyond the *h*-BN grain surface or boundary. Figure 2e shows the [0002]-projected selected area electron diffraction (SAED) pattern of the *h*-BN covered by graphene sheets taken from Figure.2d. The pattern reveals the typical hexagonal crystalline structure of *h*-BN and polycrystal of graphene, allowing us to label the peaks with the Miller–Bravais (*hkil*) indices. The distinct (0002) reflection ring (spacing ca. 0.34 nm) corresponding to graphene layer indicates the high quality of graphene sheets grown on *h*-BN. The high resolution TEM of edges of graphene obviously confirmed that the graphene sheets are few-layer (less than five), as shown in Figure 2f. Additional TEM images of few-layer graphene are shown in the Supporting Information, Figure S2. The ratio of graphene and *h*-BN can be tuned by adjusting the concentration of PMMA. When the concentration of PMMA was reduced to 2 wt %, the *h*-BN substrate was not completely covered by graphene sheets (shown in Figure S3 in the Supporting Information). When the concentration of PMMA was increased to 6 wt %, many amorphous carbon arise on the *h*-BN which is confirmed by Raman spectra discussed below (shown in Figure S4 in the Supporting Information).

Because the lattice mismatch between graphene and *h*-BN is only less than 2%,[15] it is highly possible that the origin of graphene domain is a formation growth along the plane of *h*-BN substrate. The freshly formed graphene domain has highly active edges to receive nascent carbon atoms from the decomposition of PMMA to grow up and beyond the substrate without the assistance of substrate and catalysts. The imperfect and unstable carbon sites on the substrate can be etched by the decomposed hydrogen and oxygen atoms.[14] According to the formation mechanism, high-quality graphene directly grown on *h*-BN flakes can be obtained.

Raman spectroscopy is a powerful nondestructive tool to further evaluate the thickness and quality of graphene grown on *h*-BN, as shown in Figure 3a. The *h*-BN/graphene (*h*-BN/G) composite derived from 4 wt % PMMA has a G band at 1583 cm^{-1} and a 2D band at 2685 cm^{-1}; the full-width at half-height maximum (fwhm) of the 2D band is about 61 cm^{-1}, and the intensity ratio I_{2D}/I_G is ~0.6; these results indicate that the thickness of graphene sheet is less than five.[25,26] This result agrees well with HRTEM results. The defect-related D peak at ~1340 cm^{-1} is mainly derived from defects or edges of graphene.[27,28] For *h*-BN/G derived from 2 wt.% PMMA, the shoulder peak of the D band (~1360 cm^{-1}) is the characteristic peak of the *h*-BN which is consistent with the Raman spectrum of *h*-BN as shown in Figure S4 in the Supporting Information.

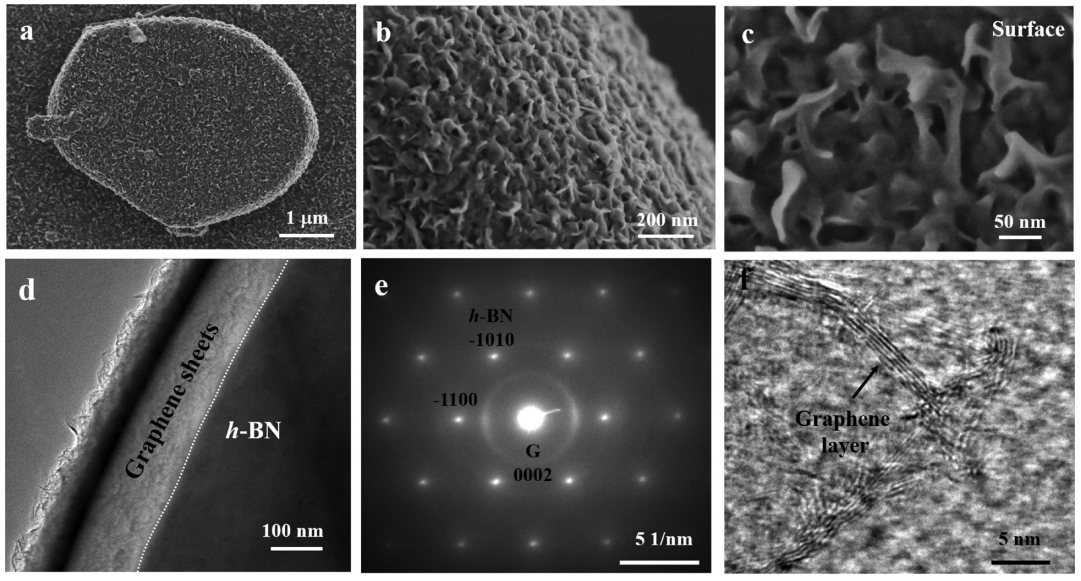

Figure 2. (a–c) SEM images of graphene directly grown on *h*-BN crystal flakes. (d) TEM images of graphene sheets growth around *h*-BN flakes, (e) SAED pattern of *h*-BN/graphene taken from d, (f) HRTEM image of edges of graphene layer.

dx.doi.org/10.1021/am405689r | ACS Appl. Mater. Interfaces 2014, 6, 3088–3092

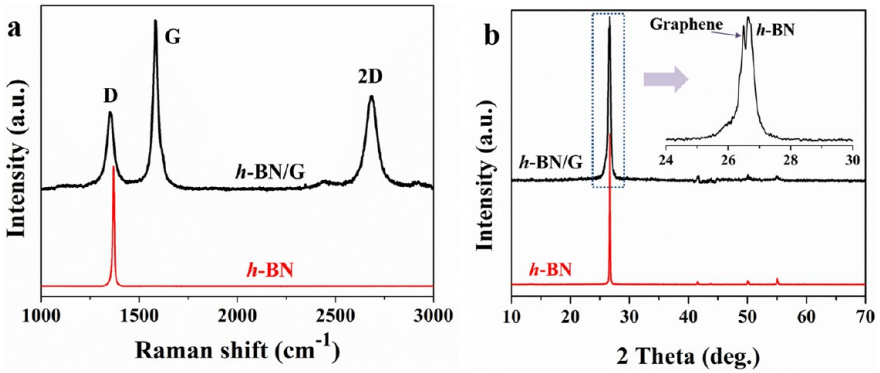

Figure 3. (a) Raman spectrum of few-layer graphene directly grown on *h*-BN substrate (*h*-BN/G) derived from 4 wt % PMMA using green (λ = 532 nm) laser excitation with laser power of 8 mW. (b) XRD patterns of *h*-BN flakes and *h*-BN/G derived from 4 wt % PMMA. The inset is enlarged region taken from *h*-BN/G.

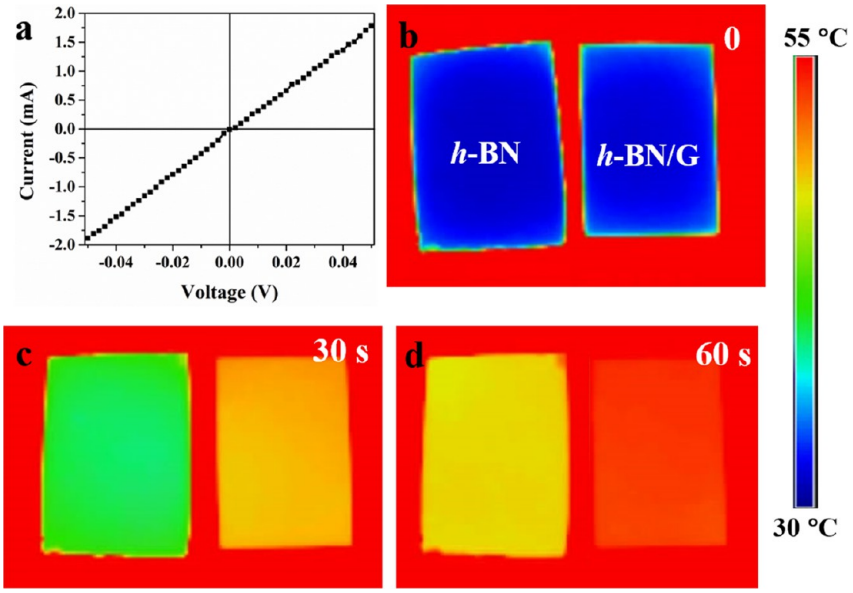

Figure 4. (a) Electrical characterization of graphene directly grown on *h*-BN showing linear (Ohmic) behavior. (b–d) Thermal transport evolution of the *h*-BN and *h*-BN/G ceramic derived from 4 wt % PMMA samples.

This result further confirmed the graphene did not completely cover the *h*-BN substrate. For *h*-BN/G derived from 6 wt.% PMMA, there shows a weak 2D peak and a strong D peak derived from disorder or defects, which indicates many amorphous carbon species exist. An additional peak arises at 26.35° in X-ray diffraction (XRD) pattern corresponding to few-layer graphene (0002) plane shown in Figure 3b. This result further confirms that highly crystalline graphene sheets can be obtained by microwave synthesis.

The growth of high-quality graphene on *h*-BN results in significant enhancement of the electrical and thermal properties. The electrical characteristics of the graphene hold the key for their future applications in devices. To evaluate the electrical conductivity, we fabricated *h*-BN/G films by vacuum filtration of colloidal dispersions of *h*-BN/G through an Anodisc membrane filter. As-prepared *h*-BN/G was dispersed in deionized water and the concentration was about 0.1 g L^{-1}. After bath sonication for 30 min, *h*-BN/G suspension was filtered to form an *h*-BN/G-filter membrane (see Figure S5 in the Supporting Information). The electrical conductivity of our *h*-BN/G film was measured by a four-probe setup, and each sample was measured three times to obtain an average value. The current–voltage (I–V) characteristic (Figure 4a) for *h*-BN/G derived from 4 wt % PMMA displays an Ohmic contact with a low sheet resistance (~46 Ω sq^{-1}), which belongs to the best ranks of graphene films and carbon nanotube films.[29,30] What's more, we can control the electrical conductivity of our *h*-BN/G films from insulator to good conductor by tuning the PMMA concentration. The pure *h*-BN is an insulator, whereas the *h*-BN/G films have sheet resistances of 339 Ω sq^{-1} with 2 wt % PMMA and 46 Ω sq^{-1} with 4 wt % PMMA. Finally, we examined the practical benefits of growing graphene on *h*-BN by measuring its thermal conductivity. In order to evaluate the thermal properties, the *h*-BN/G was compressed to form ceramic at 10 MPa by hydraulic press. The thermal conductivity of *h*-BN/G ceramic is enhanced significantly from 5.4 W m^{-1} K^{-1} for pristine *h*-BN ceramic to 9.6 W m^{-1} K^{-1} for *h*-BN/G derived from 2 wt % PMMA and to 29.1 W m^{-1} K^{-1} for *h*-BN/G derived from 4 wt % PMMA. The thermal conductivity of *h*-BN/G derived from 4 wt.% PMMA is higher than that of graphene-based composite previously reported (<10 W m^{-1} K^{-1}).[10,12,31] The increased thermal transport property of *h*-BN/G is clearly illustrated by the thermal images. Temperature distribution images of the *h*-BN and *h*-BN/G derived from 4 wt

dx.doi.org/10.1021/am405689r | ACS Appl. Mater. Interfaces 2014, 6, 3088–3092

% PMMA at 0, 30, and 60 s are shown in Figure 4b–d, respectively. The color of *h*-BN/G changed quickly from blue to red, faster than that of *h*-BN, which illustrates the graphene obviously improves the thermal transport of *h*-BN.

In summary, direct graphene growth on *h*-BN without using any catalysts is realized by a household microwave synthesis for only 5 min. The novel hybrid consisting of *h*-BN and flower-like graphene displays Ohmic contact with a low sheet resistance (~46 Ω sq^{-1}) and exhibits a very high thermal conductivity (29.1 W m^{-1} K^{-1}). The excellent properties of *h*-BN/G hybrid makes it suitable for an application as a filler of thermal conductive adhesive for the electronic industry and other applications with high electronic or thermal conductivity.

■ ASSOCIATED CONTENT

Ⓢ Supporting Information

SEM image of the *h*-BN flakes and *h*-BN/G derived from 2 wt % PMMA, TEM image of the graphene nanosheets growth on *h*-BN. This material is available free of charge via the Internet at http://pubs.acs.org.

■ AUTHOR INFORMATION

Corresponding Author

*E-mail: huangfq@mail.sic.ac.cn. Phone: 86 21 52411620.

Notes

The authors declare no competing financial interest.

■ ACKNOWLEDGMENTS

Single-crystal flakes from Momentive Performance Materials Inc, USA is highly appreciated. This work is financially supported by the Graphene Project of CAS (Grant KGZD-EW-303), the NSF of China (Grants 51125006, 91122034, 61376056, 51202274, 11274328, 51202275).

■ REFERENCES

(1) Ishida, H.; Rimdusit, S. Very High Thermal Conductivity Obtained by Boron Nitride-Filled Polybenzoxazine. *Thermochim. Acta* **1998**, *320*, 177–186.

(2) Sichel, E. K.; Miller, R. E.; Abrahams, M. S.; Buiocchi, C. J. Heat Capacity and Thermal Conductivity of Hexagonal Pyrolytic Boron Nitride. *Phys. Rev. B* **1976**, *13*, 4607–4611.

(3) Zhou, W.; Qi, S.; An, Q.; Zhao, H.; Liu, N. Thermal Conductivity of Boron Nitride Reinforced Polyethylene Composites. *Mater. Res. Bull.* **2007**, *42*, 1863–1873.

(4) Agrawal, R.; Nieto, A.; Chen, H.; Mora, M.; Agarwal, A. Nanoscale Damping Characteristics of Boron Nitride Nanotubes and Carbon Nanotubes Reinforced Polymer Composites. *ACS Appl. Mater. Interfaces* **2013**, *5*, 12052–12057.

(5) Balandin, A. A. Thermal Properties of Graphene and Nanostructured Carbon Materials. *Nat. Mater.* **2011**, *10*, 569–581.

(6) Balandin, A. A.; Ghosh, S.; Bao, W.; Calizo, I.; Teweldebrhan, D.; Miao, F.; Lau, C. N. Superior Thermal Conductivity of Single-Layer Graphene. *Nano Lett.* **2008**, *8*, 902–907.

(7) Bi, H.; Zhao, W.; Sun, S.; Cui, H.; Lin, T.; Huang, F.; Xie, X.; Jiang, M. Graphene Films Decorated with Metal Sulfide Nanoparticles for Use as Counter Electrodes of Dye-Sensitized Solar Cells. *Carbon* **2013**, *61*, 116–123.

(8) Lin, T.; Chen, J.; Bi, H.; Wan, D. Y.; Huang, F.; Xie, X. M.; Jiang, M. Facile and Economical Exfoliation of Graphite for Mass Production of High-Quality Graphene Sheets. *J. Mater. Chem. A* **2013**, *1*, 500–504.

(9) Lin, T.; Huang, F.; Liang, J.; Wang, Y. A Facile Preparation Route for Boron-Doped Graphene and Its Cdte Solar Cell Application. *Energy Environ. Sci.* **2011**, *4*, 862–865.

(10) Zhou, M.; Lin, T.; Huang, F.; Zhong, Y.; Wang, Z.; Tang, Y.; Bi, H.; Wan, D.; Lin, J. Highly Conductive Porous Graphene/Ceramic Composites for Heat Transfer and Thermal Energy Storage. *Adv. Funct. Mater.* **2013**, *23*, 2263–2269.

(11) Xue, J.; Sanchez-Yamagishi, J.; Bulmash, D.; Jacquod, P.; Deshpande, A.; Watanabe, K.; Taniguchi, T.; Jarillo-Herrero, P.; LeRoy, B. J. Scanning Tunnelling Microscopy and Spectroscopy of Ultra-Flat Graphene on Hexagonal Boron Nitride. *Nat. Mater.* **2011**, *10*, 282–285.

(12) Zhong, Y.; Zhou, M.; Huang, F.; Lin, T.; Wan, D. Effect of Graphene Aerogel on Thermal Behavior of Phase Change Materials for Thermal Management. *Sol. Energy Mater. Sol. C.* **2013**, *113*, 195–200.

(13) Ci, L.; Song, L.; Jin, C.; Jariwala, D.; Wu, D.; Li, Y.; Srivastava, A.; Wang, Z. F.; Storr, K.; Balicas, L.; Liu, F.; Ajayan, P. M. *Nat. Mater.* **2010**, *9*, 430–435.

(14) Lin, T.; Wang, Y.; Bi, H.; Wan, D.; Huang, F.; Xie, X.; Jiang, M. Atomic Layers of Hybridized Boron Nitride and Graphene Domains. *J. Mater. Chem.* **2012**, *22*, 2859–2862.

(15) Giovannetti, G.; Khomyakov, P. A.; Brocks, G.; Kelly, P. J.; van den Brink, J. Substrate-Induced Band Gap in Graphene on Hexagonal Boron Nitride: AB Initio Density Functional Calculations. *Phys. Rev. B* **2007**, *76*, No. 073103.

(16) Bjelkevig, C. Electronic Structure of a Graphene/Hexagonal-BN Heterostructure Grown on Ru (0001) by Chemical Vapor Deposition and Atomic Layer Deposition: Extrinsically Doped Graphene. *J. Phys.: Condens. Matter.* **2010**, *22*, No. 302002.

(17) Oshima, C.; Itoh, A.; Rokuta, E.; Tanaka, T.; Yamashita, K.; Sakurai, T. A Hetero-Epitaxial-Double-Atomic-Layer System of Monolayer Graphene/Monolayer *h*-BN on Ni (111). *Solid State Commun.* **2000**, *116*, 37–40.

(18) Panda, A. B.; Glaspell, G.; El-Shall, M. S. Microwave Synthesis of Highly Aligned Ultra Narrow Semiconductor Rods and Wires. *J. Am. Chem. Soc.* **2006**, *128*, 2790–2791.

(19) Dong, C.; Guo, J.; Fu, G.; Yang, L.; Chen, H. Rapid Preparation of MgB_2 Superconductor Using Hybrid Microwave Synthesis. *Supercond. Sci. Technol.* **2004**, *17*, L55.

(20) Agrawal, D. K. Microwave Processing of Ceramics. *Curr. Opin. Solid State Mater. Sci.* **1998**, *3*, 480–485.

(21) Brunetti, F. G.; Herrero, M. A.; Muñoz, J. d. M.; Díaz-Ortiz, A.; Alfonsi, J.; Meneghetti, M.; Prato, M.; Vázquez, E. Microwave-Induced Multiple Functionalization of Carbon Nanotubes. *J. Am. Chem. Soc.* **2008**, *130*, 8094–8100.

(22) Hassan, H. M. A.; Abdelsayed, V.; Khder, A. E. R. S.; AbouZeid, K. M.; Terner, J.; El-Shall, M. S.; Al-Resayes, S. I.; El-Azhary, A. A. Microwave Synthesis of Graphene Sheets Supporting Metal Nanocrystals in Aqueous and Organic Media. *J. Mater. Chem.* **2009**, *19*, 3832–3837.

(23) Janowska, I.; Chizari, K.; Ersen, O.; Zafeiratos, S.; Soubane, D.; Costa, V.; Speisser, V.; Boeglin, C.; Houllé, M.; Bégin, D.; Plee, D.; Ledoux, M.-J.; Pham-Huu, C. Microwave Synthesis of Large Few-layer Graphene Sheets in Aqueous Solution of Ammonia. *Nano Res.* **2010**, *3*, 126–137.

(24) Sharma, S.; Ganguly, A.; Papakonstantinou, P.; Miao, X.; Li, M.; Hutchison, J. L.; Delichatsios, M.; Ukleja, S. Rapid Microwave Synthesis of CO Tolerant Reduced Graphene Oxide-Supported Platinum Electrocatalysts for Oxidation of Methanol. *J. Phys. Chem. C* **2010**, *114*, 19459–19466.

(25) Ferrari, A. C.; Meyer, J. C.; Scardaci, V.; Casiraghi, C.; Lazzeri, M.; Mauri, F.; Piscanec, S.; Jiang, D.; Novoselov, K. S.; Roth, S.; Geim, A. K. Raman Spectrum of Graphene and Graphene Layers. *Phys. Rev. Lett.* **2006**, *97*, No. 187401.

(26) Ferrari, A. C. Raman Spectroscopy of Graphene and Graphite: Disorder, Electron–Phonon Coupling, Doping and Nonadiabatic Effects. *Solid State Commun.* **2007**, *143*, 47–57.

(27) Jeon, I. Y.; Shin, Y. R.; Sohn, G.-J.; Choi, H.-J.; Bae, S. Y.; Mahmood, J.; Jung, S. M.; Seo, J.-M.; Kim, M.-J.; Chang, D. W.; Dai, L.; Baek, J. B. Edge-Carboxylated Graphene Nanosheets Via Ball Milling. *P. Natl. Acad. Sci. USA.* **2012**, *109*, 5588–5593.

(28) Lin, T.; Tang, Y.; Wang, Y.; Bi, H.; Liu, Z.; Huang, F.; Xie, X.; Jiang, M. Scotch-Tape-Like Exfoliation of Graphite Assisted with Elemental Sulfur and Graphene-Sulfur Composites for High-Performance Lithium-Sulfur Batteries. *Energy Environ. Sci.* **2013**, *6*, 1283−1290.
(29) Talapatra, S.; Kar, S.; Pal, S. K.; Vajtai, R.; Ci, L.; Victor, P.; Shaijumon, M. M.; Kaur, S.; Nalamasu, O.; Ajayan, P. M. Direct Growth of Aligned Carbon Nanotubes on Bulk Metals. *Nat. Nanotechnol.* **2006**, *1*, 112−116.
(30) Rao, R.; Chen, G.; Arava, L. M. R.; Kalaga, K.; Ishigami, M.; Heinz, T. F.; Ajayan, P. M.; Harutyunyan, A. R. Graphene as an Atomically Thin Interface for Growth of Vertically Aligned Carbon Nanotubes. *Sci. Rep.* **2013**, *3*, No. 1891.
(31) Zhou, M.; Bi, H.; Lin, T.; Lu, X.; Huang, F.; Lin, J. Directional Architecture of Graphene-Ceramic Composites with Improved Thermal Conduction for Thermal Applications. *J. Mater. Chem. A* **2014**, *2*, 2187−2193.